



Green Synthesis, Texture, Electron Diffraction, Thermal and Optical Properties of Cobalt Doped Arginine Carbon Nanotubes

SARVESH KUMAR SHAIKESH^{1,*}, B. TIWARI² and K. YADAV³

¹Department of Chemistry, Lalit Narayan Mithila University, Darbhanga-846004, India

²Department of Chemistry, D.S. Institute of Technology & Management, Ghaziabad-201017, India

³Department of Chemistry, Samastipur College, Samastipur-848134, India

*Corresponding author: E-mail: skshailesh07@gmail.com

Received: 19 February 2021;

Accepted: 16 March 2021;

Published online: 16 April 2021;

AJC-20333

In this work, a simple and viable method of green synthesis of multi-walled cobalt doped arginine carbon nanotubes (CNT's) by chemical precipitation method using arginine amino acid is reported. The atomic force microscopy confirmed that metal ions present in a branched fashion on the surface of Co-doped arginine CNT's and the obtained particle with diameter 20 nm well dispersed on the carbon nanotubes. The TEM analysis indicates the interlayer separation between the two adjacent carbon walls is estimated to be about 0.34 nm. The electron diffraction patterns indicate that the tube has nearly identical chirality for all of the concentric graphitic layers, as a zigzag-type MWCNT. The SEM analysis predicted tube like morphology and strain is existed on the surface of the CNTs. The Raman spectra confirmed the armchair ($n = 8$ to 11) multi-walled nanotubes with this chirality are assigned as a semiconducting type of nanotubes. The thermal property was studied by thermogravimetric analysis, differential thermal analysis and predicted the 27.81 % purity in CNTs.

Keywords: Cobalt-Arginine complex, Encapsulated, Dendrimer, Armchair, Raman spectra.

INTRODUCTION

Carbon nanotubes have adhered a considerable enchant in the contemporaneous situation because of its unique chemical properties, like high specific surface area [1], chemical stability, thermal conductivity [2,3], optical [4], mechanical [5,6] and electrical properties. It is considered as one of the alternative area for replacing traditional conventional processes with this new emerging science aimed at miniaturizing of processes with almost efficient uses compared to others. It consists of graphite [7] like carbon, having a length of 1-100 nm and a diameter up to several micrometers or even up to millimeters. The transition size from micro to the nano leads to the number of changes in physical properties and chemical properties.

When CNT's is converted into the nanosize, the surface to the volume area is increased [8], and thus creates more sites for the bonding, catalysis, resulted in the increased strength and chemical or heat resistance [9-14]. They are among the stringent [15-18], indestructible fiber [19] and have astonishing electronic properties [20-22] with many other unique properties.

Carbon nanotubes have a broad range of potential diligence [23-25] in nanoelectronics [26,27] gas sensors [28], cancer therapy [29] and diagnoses. Due to huge application of CNT's, it is required to develop new economical methods and techniques to prepare carbon nanotubes and characterized them. For the economical production of carbon nanotubes amino acid, fatty acid, natural product, cytochrome, ferredoxin source can be taken as the key material. It is also required to inculcate some desired properties in them, so that they can be used in various applications.

In present work, a novel cobalt-doped arginine multi-walled carbon nanotubes were prepared using cobalt ions and arginine separated from the egg protein and characterized by AFM, SEM, TEM, Raman and thermal techniques.

EXPERIMENTAL

All the chemicals used in the synthesis were of A.R. grade. Surface characterization was performed by TEM (TEM-TECNAI G.2.20 S-TWIN, Netherlands) and atomic force microscopy (NTEGRA Prima, NT-MDT, Moscow, Russia). The surface

images of multi-walled carbon nanotubes were obtained using the scanning electron microscopy NovaNano SEM 450 (FEI, Eindhoven, Netherlands). Thermal analysis (TG/TGA, DTA and DTG) was conducted on Perkin-Elmer Pyris diamond instrument.

Preparation of CNTs in aqueous medium by arginine cobalt complex: The preparation of Co-doped arginine carbon nanotubes was taken place by treating 1 N $\text{Co}(\text{NO}_3)_2$ solution with the arginine separated from the egg protein. Arginine comprises of amino acid as a monomer, when reacted with alcoholic solution of Co^{2+} resulted in the formation of the complex. The solid complex was filtered and washed with 1 N HCl solution to remove the excess metal ions from the surface. In order to obtain MWCNT's, the complex was decomposed at 600 °C [30,31].

RESULTS AND DISCUSSION

AFM studies: Atomic force microscopy (AFM) images confirmed the maximum peak height is around 179.25 nm. The evaluation of the results confirmed the synthesized CNT's are multiwalled and the particle size is around 20 nm. The maximum peak height obtained is of 179.25 nm with no peaks in between. The distance between peak to peak in y-direction is 179 nm and in z-direction is 89.78 nm as shown in Fig. 1b. The average sizes of peaks are 101.38 nm and the roughness of the synthesized nanoparticle is ~ 20.93 nm. The skewness (Rsk) measures the degree of asymmetry of surface height distribution, which was found to be in the range of -0.1049. A negative value of Rsk indicates that the surface contains the cracks, group of valleys and planar type of structure. Therefore a negatively skewed surface is good for surface in proximity and moving relative to each other. It encapsulated the load bearing capacity, void fraction and characteristics of non-traditional mashing processes. Kurtosis is a measure of the dissemination of sharp point above and below the mean line. Coefficient of kurtosis is -0.1521, which indicates the surface is uneven with many patches raised above the surface as the value of kurtosis is less than 3.

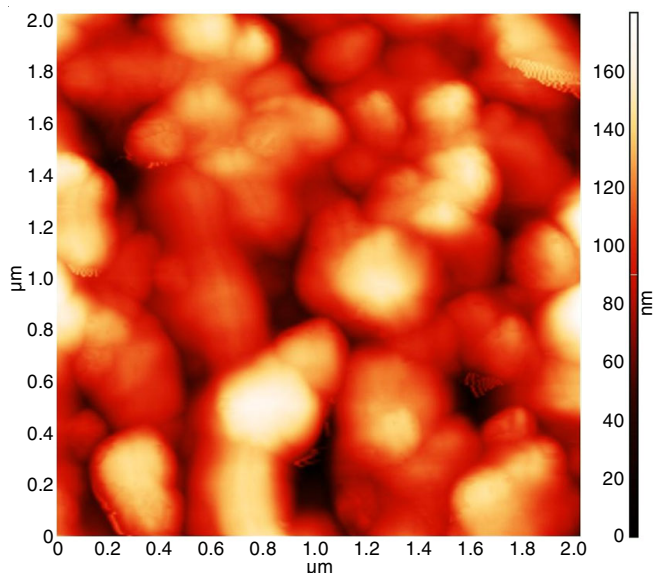


Fig. 1a. AFM image of cobalt doped arginine carbon nanotubes showing linear dendritic form

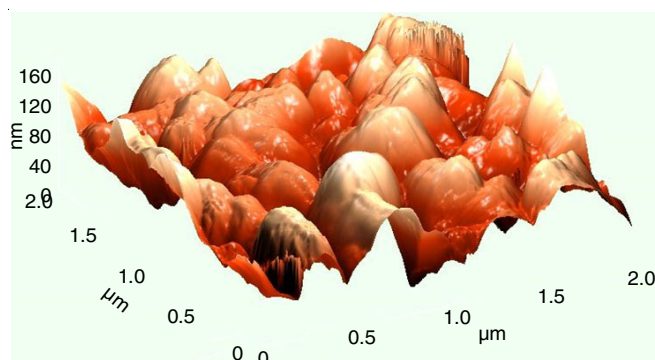


Fig. 1b. 3D morphology of cobalt doped arginine carbon nanotubes

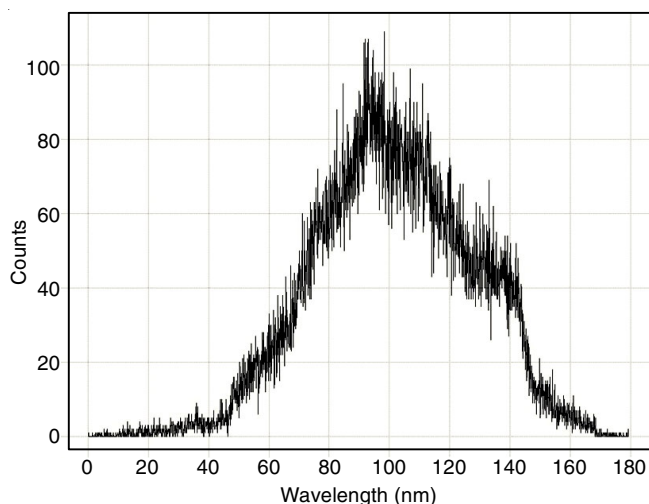


Fig. 1c. The roughness by the out XEI's park system

TEM studies: TEM image (Fig. 2a) predicted that synthesized MWCNTs has the outer diameter range of 6-60 nm and their walls consisted of several graphitic layers which was apared by 0.36 nm. These results confirmed the existance of chirality in the nanotubes. The electron diffraction patterns were overlapped due to two simple hexagonal patterns, which indicated that all layers in the MWCNT have nearly identical chirality. The diffraction patterns closely exhibited the center of symmetry, which suggested the presence of well-defined shuffle in these nanotubes. The inspection of (101) reflections shows that the positional correlation between the internal structures of the nanotubes walls has a tendency of AB arrangement. In addition to the sharp (0002) and (1010) reflections, (1011) grid edging become visible, which results from the bent graphitic sheets. A fast Fourier transformation (FFT) from the walls of the nanotube obviously exhibits (1011) lattice fringes.

Fig. 2b shows the three electron diffraction patterns in which the nanotube axis is vertical. The short smooth curving line clearly showed the actuality of graphene layer with respect to vertical tube axis. However, diffraction pattern from the plane in the forms {100} and {110} shows the radii corresponding to d-spacing of 0.209 and 0.123 nm, respectively.

SEM studies: Morphology and size of the material were investigated using Scanning electron microscope (SEM) at 20.0 kV and 15 A current having magnification at 200000x. The SEM micrograph of MWCNT's (Fig. 3) shows the full of pores

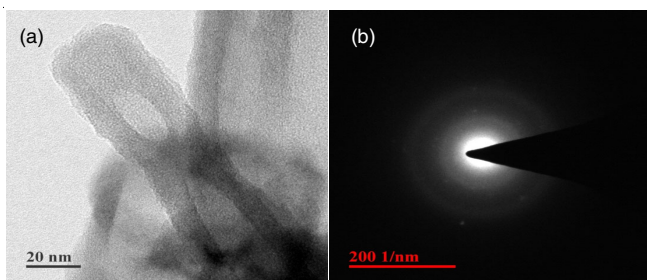


Fig. 2. (a) TEM images of carbon nanotubes synthesized on decomposition of cobalt arginine complex, (b) Electron diffraction of the carbon nanotubes

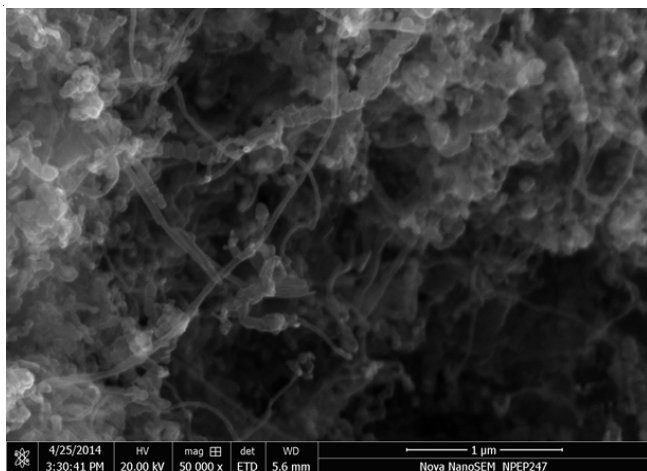


Fig. 3. SEM images of carbon nanotubes synthesized at decomposition of cobalt arginine complex

and layered structure of nanotubes having large pile of things arranged one on top of other consisting of hundreds of carbon nanosheets. It was also analyzed that the surface of the carbon nanotubes were in the zig-zag fashion, which clearly indicated that the nanocomposite consists of extremely fine particles with ribbon-like structure that make heavier as close proximity due to the extremely small surface and high surface energy of the obtained nanoparticles. The SEM images also shows that Co doped carbon nanosheets were decorated with the spherical Co and minerals, which are homogeneously distributed on the surface of graphene sheets.

A close examination predicted the frangible crack, which could be due to the elastic stress present on the exterior of the material and usually propagates at high velocity, sometimes with little associated absorbed free energy. The appearance of metallic surface defects results in the breakage of more than one crystallographic plane within a particular particle, leading to the brittleness of the material. These lines pattern were formed by a ductile process, however due to the creation of non-resolvable slip deformation such fracture cannot be considered as quasi-cleavage. Alternatively, with less constraint, the connecting ligaments may become sufficiently large as the homogenized micro void was observed in thin bands were merged through the general cleavage surface.

Raman studies: Fig. 4 shows a shakiness at the absolute frequency peak around 200 cm^{-1} , which is designated to the A_{1g} symmetry radial breathing mode. This peak was absent in

the other carbon materials, which is the main configuration of the CNTs. A clear identification of the radial breathing modes of MWCNTs with thin layer inner concentric ring was also observed. The Raman spectra established that these modes agreed with the restricted Boltzmann machines (RBMs), which originate from the straitened innermost graphitic layers. The peak around 1350 cm^{-1} is designated to the D-band, due to the presence of disarray in the concentric graphitic inner layer of nanotubes. The result also demonstrated that D band is active in the nanotubes exhibiting chirality due to the double resonance condition. The peaks around $1600\text{--}1550\text{ cm}^{-1}$ is designated to the G-band. The peak at 1585 cm^{-1} describes the tangential vibrations of the carbon atoms and coincides with the graphitic carbon atom. In carbon nanotubes, the G-band is composed of two features (G+ and G-) due to the impoundment of the reciprocating wave near the circumference. The G+ band coherent with atomic expatriation along the nanotube axis is independent of the diameter, as antagonistic to the G-band, which compatible to circumferential atomic displacements. If single peak existed in the RBM mode and multiple peak in the G band is expressed by the surface enhanced Raman scattering (SERS). The SERS results were implied by assigning G-band modes from the innermost layer and a graphitic carbon from the outermost layer in the MWCNT. The peak around 2700 cm^{-1} is designated as a overtone or second-order harmonic of the D* or 2D. The D* or 2D band is emblematic of second-order scattering process which results in the creation of an inelastic quantum of energy associated with the compressional wave. The unique feature at 890 cm^{-1} , which is concomitant with arm-chair ($n = 8$ to 11) multi-walled nanotubes. The armchair with this property of asymmetry is designated as the semiconducting type of characteristics in the nanotubes.

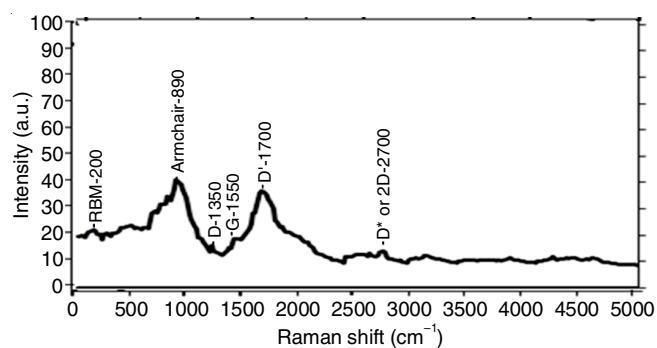


Fig. 4. Raman spectra of carbon nanotubes

Thermal analysis: Thermogravimetric analysis was performed on the samples to determine the stability, purity and humidity. The thermogram calculated the 62.19% mass decomposition of metal ion in CNTs from $21\text{--}1379\text{ }^{\circ}\text{C}$ and also 27.81% metal purity in CNTs, which proved the high thermal stability of CNT's.

In Fig. 5, blue line at $100\text{ }^{\circ}\text{C}/\text{min}$ indicates a small loss in weight sample with the increase temperature. The decomposition of the complex take place at a very slower rate of 3% loss in weight per $100\text{ }^{\circ}\text{C}$ increase in temperature up to $900\text{ }^{\circ}\text{C}$ and in the temperature range of $900\text{--}1300\text{ }^{\circ}\text{C}$, the decomposition

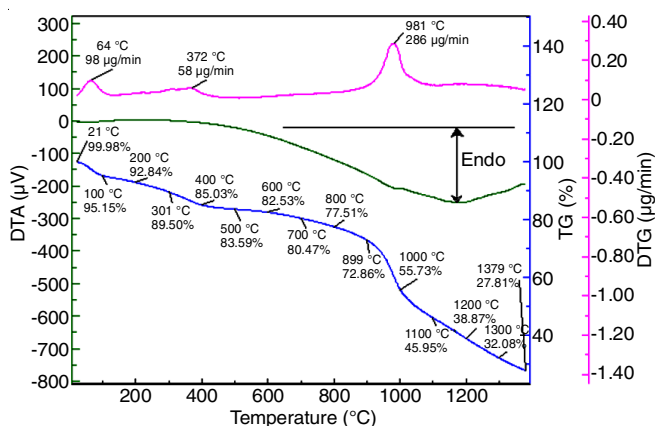


Fig. 5. TGA, DTG and DTA image of carbon nanotubes by the arginine cobalt complex

rate increases to 10% per 100 °C increase of temperature. The DTA analysis of the prepared CNT shown by green line in Fig. 5 shows the differential temperature plotted against temperature. In the first region (0-500 °C), the sample shows that the material is stable upto 500 °C, the analysis shows that the peak shows a major endotherm at 1200 °C, which is about 65 °C below that of the major peak due to reduction of cobalt-arginine complex. The material shows a sharp transition in its heat content due sharp change in its solubility. The overall thermal observation shows that CNT behaves as a good conductor even at high temperature range. From the DTG, it can be predicted that the mass loss is more in the 700-1000 °C range, as dm_i/dT_i slope is high for this region, otherwise at other temperatures the curve is nearly flat below 700 °C, shows its high thermal stability.

Conclusion

Multiwalled cobalt doped arginine carbon nanotubes were prepared by the decomposition of cobalt-arginine complex. The TEM analysis confirmed that the diameter of the particle in the range of 10-20 nm and also predicted the zigzag dendrimer shape. The SEM analysis predicted the multivalued structure of carbon nanotubes and particle size is 20 nm. The TGA analysis showed that the 62.19% mass decomposition of metal ion in CNTs from 21-1379 °C. The presence of 27.81% metal purity in CNTs proved the high thermal stability of CNTs. The DTA analysis of the sample showed that the prepared material was very stable up to 500 °C, which also shows a major endothermic peak at 1200 °C which is about 65 °C below that of the major peak because of the reduction of arginine complex. In the Raman spectra, two peak namely G (graphite), D (disorder) and their second-order harmonic (G' band), explicitly appears at ~1670, ~1320 and ~2750 cm^{-1} , respectively confirmed the nanostructure. The another interesting feature of Raman spectra at 890 cm^{-1} , which is associated with armchair ($n = 8$ to 11) multi-walled nanotubes. The armchair nanotubes with this chirality were designated as a semiconducting type of nanotubes.

ACKNOWLEDGEMENTS

The authors are thankful to Institute Instrumentation Centre, IIT Roorkee, Roorkee, India for providing the spectral and analytical data.

CONFLICT OF INTEREST

The authors declare that there is no conflict of interests regarding the publication of this article.

REFERENCES

- C.N.R. Rao, G.U. Kulkarni, P.J. Thomas and P.P. Edwards, *Chem. Eur. J.*, **8**, 28 (2002); [https://doi.org/10.1002/1521-3765\(20020104\)8:1<28::AID-CHEM28>3.0.CO;2-B](https://doi.org/10.1002/1521-3765(20020104)8:1<28::AID-CHEM28>3.0.CO;2-B)
- S.C. Tsang, Y.K. Chen, P.J.F. Harris and M.L.H. Green, *Nature*, **372**, 159 (1994); <https://doi.org/10.1038/372159a0>
- E. Dujardin, T.W. Ebbesen, T. Hiura and K. Tanigaki, *Science*, **265**, 1850 (1994); <https://doi.org/10.1126/science.265.5180.1850>
- H. Ago, K. Petritsch, M.S.P. Shaffer, A.H. Windle and R.H. Friend, *Adv. Mater.*, **11**, 1281 (1999); [https://doi.org/10.1002/\(SICI\)1521-4095\(199910\)11:15<1281::AID-ADMA1281>3.0.CO;2-6](https://doi.org/10.1002/(SICI)1521-4095(199910)11:15<1281::AID-ADMA1281>3.0.CO;2-6)
- M.-F. Yu, *J. Eng. Mater. Technol.*, **126**, 271 (2004); <https://doi.org/10.1115/1.1755245>
- M.R. Falvo, G.J. Clary, R.M. Taylor II, V. Chi, F.P. Brooks Jr., S. Washburn and R. Superfine, *Nature*, **389**, 582 (1997); <https://doi.org/10.1038/39282>
- M.S. Dresselhaus, G. Dresselhaus and P.C. Eklund, *Science of Fullerenes and Carbon Nanotubes*, Academic Press (1996).
- G. Hodes, *Adv. Mater.*, **19**, 639 (2007); <https://doi.org/10.1002/adma.200601173>
- T. Tsoufis, A. Tomou, D. Gournis, A.P. Douvalis, I. Panagiotopoulos, B. Kooi, V. Georgakilas, I. Arfaoui and T. Bakas, Thomas, *J. Nanosci. Nanotechnol.*, **8**, 5942 (2008); <https://doi.org/10.1166/jnn.2008.18366>
- V. Georgakilas, V. Tzitzios, D. Gournis and D. Petridis, *Chem. Mater.*, **17**, 1613 (2005); <https://doi.org/10.1021/cm0483590>
- S.J. Liu, C.H. Huang, C.K. Huang and W.S. Hwang, *Chem. Commun.*, **32**, 4809 (2009); <https://doi.org/10.1039/b908534c>
- Y. Sun and Y. Xia, *Science*, **298**, 2176 (2002); <https://doi.org/10.1126/science.1077229>
- C.J. Murphy, T.K. Sau, A.M. Gole, C.J. Orendorff, J. Gao, L. Gou, S.E. Hunyadi and T. Li, *J. Phys. Chem. B*, **109**, 13857 (2005); <https://doi.org/10.1021/jp0516846>
- Y. Xia, P. Yang, Y. Sun, Y. Wu, B. Mayers, B. Gates, Y. Yin, F. Kim and H. Yan, *Adv. Mater.*, **15**, 353 (2003); <https://doi.org/10.1002/adma.200390087>
- S. Kunze, R. Hohmann, H.-J. Kluge, J. Lantzsch, L. Monz, J. Stenner, K. Stratmann, K. Wendt and K. Zimmer, *Z. Phys. D-Atoms Molecules and Clusters*, **27**, 111 (1993); <https://doi.org/10.1007/BF01426757>
- B.I. Yakobson, C.J. Brabec and C.J. Bernholc, *Phys. Rev. Lett.*, **76**, 2511 (1996); <https://doi.org/10.1103/PhysRevLett.76.2511>
- M.M.J. Treacy, T.W. Ebbesen and J.M. Gibson, *Nature*, **381**, 678 (1996); <https://doi.org/10.1038/381678a0>
- P.E. Wong, C.M. Sheehan and C.M. Lieber, *Science*, **277**, 1971 (1997); <https://doi.org/10.1126/science.277.5334.1971>
- M.S. Dresselhaus, G. Dresselhaus, K. Sugihara, I.L. Spain and H.A. Goldberg, *Graphite Fibers and Filaments*, Springer: Berlin, Heidelberg, p. 407 (1998).
- P.G. Collins and K.M. Bradley, *Science*, **287**, 1801 (2000); <https://doi.org/10.1126/science.287.5459.1801>
- X.P. Tang, A. Kleinhammes, H. Shimoda, L. Fleming, K.Y. Bennoune, C. Bower, O. Zhou and Y. Wu, *Science*, **288**, 492 (2000); <https://doi.org/10.1126/science.288.5465.492>
- J. Kong, N.R. Franklin, C. Zhou, M.G. Chapline, S. Peng, K. Cho and H. Dai, *Science*, **287**, 622 (2000); <https://doi.org/10.1126/science.287.5453.622>

23. I. Brodie and C.A. Spindt, Vacuum Microelectronics, In: Advances in Electronics and Electron Physics, Academic Press: New York, vol. 83, pp. 1-106 (1992).
24. J.A. Castellano, Handbook of Display Technology, Academic Press: San Diego, p. 395 (1992).
25. A.W. Scott, Understanding Microwaves, Wiley, p. 395 (1993).
26. P.J. Britto, K.S.V. Santhanam, A. Rubio, A. Alonso and P.M. Ajayan, *Adv. Mater.*, **11**, 154 (1999); [https://doi.org/10.1002/\(SICI\)1521-4095\(199902\)11:2<154::AID-ADMA154>3.0.CO;2-B](https://doi.org/10.1002/(SICI)1521-4095(199902)11:2<154::AID-ADMA154>3.0.CO;2-B)
27. G. Che, B.B. Lakshmi, E.R. Fisher and C.R. Martin, *Nature*, **393**, 346 (1998); <https://doi.org/10.1038/30694>
28. J.M. Planeix, N. Coustel, B. Coq, V. Brotons, P.S. Kumbhar, R. Dutartre, P. Geneste, P. Bernier and P.M. Ajayan, *J. Am. Chem. Soc.*, **116**, 7935 (1994); <https://doi.org/10.1021/ja00096a076>
29. H. Hong, Y. Zhang, J. Sun and W. Cai, *Nano Today*, **4**, 399 (2009); <https://doi.org/10.1016/j.nantod.2009.07.001>
30. S.K. Shailesh, A.K. Roy and B. Tiwari, *Int. J. Mater. Mechan. Manufact.*, **2**, 99 (2014).
31. S.K. Shailesh, B. Tiwari, K. Yadav and D. Prakash, *Int. J. Metallur. Mater. Sci. Eng.*, **3**, 13 (2013).